FULL PAPER

Dalton
www.rsc.org/dalton

Steric effects caused by *N*-alkylation of the tripodal chelator *N*,*N*′,*N*″-tris(2-pyridylmethyl)-*cis*,*cis*-1,3,5-triaminocyclohexane (tachpyr): structural and electronic properties of the Mn(II), Co(II), Ni(II), Cu(II) and Zn(II) complexes

Gyungse Park,[a] Ann M. Przyborowska,[a] Neng Ye,[a] Nicole M. Tsoupas,[a] Cary B. Bauer,[b] Grant A. Broker,[c] Robin D. Rogers,[c] Martin W. Brechbiel[d] and Roy P. Planalp *[a]

[a] *Department of Chemistry, University of New Hampshire, Durham, NH 03824, USA. E-mail: roy.planalp@unh.edu*
[b] *Department of Chemistry, The University of Alabama, Tuscaloosa, AL 35487, USA*
[c] *Bruker AXS, Inc., 5465 East Cheryl Parkway, Madison, WI 53711, USA*
[d] *Radioimmune & Inorganic Chemistry Section, Radiation Oncology Branch, National Institutes of Health, Bethesda, MD 20892 USA*

Received 20th September 2002, Accepted 21st November 2002
First published as an Advance Article on the web 23rd December 2002

The effects of steric hindrance on the complexation of Mn(II), Co(II), Ni(II), Cu(II) and Zn(II) by chelators based on *cis*,*cis*-1,3,5-triaminocyclohexane (tach) have been studied. The chelators studied are the 2-methylpyridyl pendant-arm derivatives of tach, 'tachpyr' (*N*,*N*′,*N*″-tris(2-pyridylmethyl)-*cis*,*cis*-1,3,5-triaminocyclohexane), and the *N*-alkylated analogs '(N–Me)$_3$tachpyr' (*N*,*N*′,*N*″-trimethyl-*N*,*N*′,*N*″-tris(2-pyridylmethyl)-*cis*,*cis*-1,3,5-triaminocyclohexane) and '(N–Et)$_3$tachpyr' (*N*,*N*′,*N*″-triethyl-*N*,*N*′,*N*″-tris(2-pyridylmethyl)-*cis*,*cis*-1,3,5-triaminocyclohexane). Hexacoordinate complexes, $[M^{II}L]X_2$ resulted from reaction of the appropriate metal ion salts with L in alcoholic medium (M = Mn, Co, Ni, Cu, Zn; L = tachpyr, (N–Me)$_3$tachpyr, (N–Et)$_3$tachpyr; X = ClO_4^-, NO_3^-, Cl^-). The Mn(II) and Co(II) complexes have high-spin electron configurations, based on solution magnetic susceptibility, electronic spectral and/or X-ray crystallographic studies. However, solution visible-near IR electronic spectra and single-crystal X-ray crystallography demonstrate weakened bonding in the complexes of (N–R)$_3$tachpyr relative to tachpyr, due to steric effects of methyl or ethyl groups on coordinated tach amines. Structures of $[Zn(tachpyr)]^{2+}$ and $[Ni(tachpyr)]^{2+}$ indicate a clear preference of tachpyr and derivatives for octahedral geometry, while $[Cu((N–Me)_3tachpyr)]^{2+}$ exhibits a classic Jahn–Teller tetragonal distortion. The complex $[Mn(tachpyr)](ClO_4)_2$ demonstrates a striking influence of the metal ion on the coordination geometry, with a trigonal-prismatic coordination of Mn(II) and considerable distortion of the tach-amino donor groups. The coordination geometry and distortions are attributed to the large size of high-spin d^5 Mn(II) and the absence of ligand-field stabilization energy, coupled with the observed preference of tachpyr derivatives for octahedral geometry. The $[M^{II}(tachpyr)]^{2+}$ complexes (M = Co, Ni, Cu and Zn) are inert in aqueous pH 5.5 media. However, all metal complexes of *N*-alkylated tachpyr, as well as $[Mn(tachpyr)](ClO_4)_2$, dissociate metal ion in aqueous pH 5.5 medium, consistent with their steric hindrance and distortions respectively.

Introduction

Chelating agents have numerous medical applications, including nuclear medicine,[1,2] magnetic resonance shift reagents,[3] and the detoxification of excess metal ions.[4,5] We reported the preparation and iron-binding properties of a novel chelator, *N*,*N*′,*N*″-tris(2-pyridylmethyl)-*cis*,*cis*-1,3,5-triaminocyclohexane (tachpyr) (Scheme 1, R = H), and investigated its complexation chemistry of divalent metal ions, particularly of iron.[8,9] Interestingly, tachpyr was found to be cytotoxic to human and murine bladder tumor cells, an effect that was attributed to metal-chelating properties, with iron, zinc and copper as particular targets.[8] The Fe(II) complex [Fe(tachpyr)]-Cl$_2$ is low-spin (LS), indicative of a strong metal–ligand interaction. The interaction of tachpyr with Fe(III) or Fe(II) in the presence of O$_2$ leads to oxidative dehydrogenation of tachpyr, forming tachpyr-imino derivatives of Fe(II), typified by $[Fe(tachpyr-ox-4)]^{2+}$ (Scheme 2).[9] In order to investigate the role of oxidative dehydrogenation and steric effects on the chelating abilities of tachpyr, we prepared the *N*-alkylated derivatives of tachpyr, (N–R)$_3$tachpyr (Scheme 1, R = Me, Et), which would presumably not undergo oxidative dehydrogenation.[9] Indeed, $[Fe((N–Me)_3tachpyr)]^{2+}$ does not undergo oxidative dehydrogenation, and (N–Me)$_3$tachpyr is not cytotoxic. Moreover, $[Fe((N–Me)_3tachpyr)]^{2+}$ is a complex of high-spin (HS) Fe(II) that decomposes in anaerobic aqueous pH 7.4 media, whereas $[Fe(tachpyr)]^{2+}$ is indefinitely stable.[10] The findings indicated that the metal-binding properties of tachpyr are weakened by *N*-alkylation, likely from the steric effects of the introduced alkyl groups.

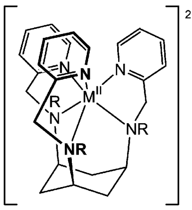

M	L tachpyr (R = H)	 (N-Me)$_3$tachpyr (R = Me)	 (N-Et)$_3$tachpyr (R = Et)
Mn(II)	**1a**	**1b**	**1c**
Co(II)	**2a**	**2b**	**2c**
Ni(II)	**3a, 3a'**	**3b**	**3c**
Cu(II)	**4a**[b]	**4b**	**4c**
Zn(II)	**5a**[b]	**5b**	**5c**

[a] The anion X = ClO_4^- with exception of **2b** where X = NO_3^-, and **3a** where X = Cl^-. [b] Previously reported.[6,7]

Scheme 1 Structure and numbering scheme of the metal complexes of tachpyr, (N–Me)$_3$tachpyr and (N–Et)$_3$tachpyr.[a]

DOI: 10.1039/b209228j

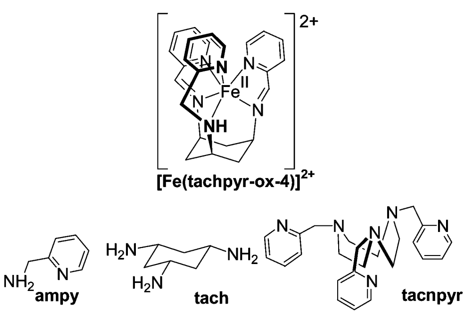

Scheme 2 Imine complex [Fe(tachpyr-ox-4)]$^{2+}$ derived from oxidation of [Fe(tachpyr)]$^{2+}$, and several chelators to be compared with tachpyr and (N–R)$_3$tachpyr.

To better define the impact of *N*-alkylation on metal complexation by tach-family chelators, we synthesized and characterized Mn(II), Co(II), Ni(II), Cu(II), and Zn(II) complexes of tachpyr and (N–R)$_3$tachpyr (R = Me, Et). Their solution and solid-state structures, and the elucidation of trends in metal binding as a function of R, are described herein.

Results and discussion

Synthesis and aqueous lability

The complexes of Scheme **1** were prepared by reactions of the respective metal salts and the ligand (1:1) in MeOH or EtOH solvents. A MeOH:Et$_2$O solvent mixture (1:2) was used in some cases to accelerate precipitation and improve yields.[11] Vapor-phase diffusion of Et$_2$O into CH$_3$CN or MeOH solutions served to purify and crystallize the complexes. A 1:1 M:L composition was verified for all products by elemental analysis and FAB-mass spectrometry. Proton NMR of the Zn(II) complexes in DMSO or aqueous pH 7.4[10] medium show characteristic changes in the cyclohexyl ring proton–proton coupling constants relative to free chelator, indicating that the tach framework assumes the 'closed' (triaxial nitrogens) conformation. The 2-pyridylmethylene protons are diastereotopic, which indicates that the three 2-pyridylmethyl arms of the Zn(II)-tachpyr complexes are static with respect to Δ–Λ interconversion, as was found for Ga(III)-tachpyr and In(III)-tachpyr derivatives.[12] Inertness of the complexes was also assessed by reversed-phase HPLC with an aqueous pH 5.5-MeOH gradient mobile phase. Single components with retention times of *ca.* 7–12 min, characteristic of dicationic tachpyr complexes,[6] were only observed for [Ni(tachpyr)]$^{2+}$ and [Co(tachpyr)]$^{2+}$. The [Co(tachpyr)]$^{2+}$ complex exhibited a second component at a 3.34 min retention time, consistent with oxidation to a Co(III) complex, which would be analogous to redox behavior of Fe-tachpyr complexes and the tendency of tachpyr-imine chelators to favor the d^6-low-spin electron configuration.[9] Chromatograms of [Mn(tachpyr)]$^{2+}$ and all complexes of the *N*-alkylated tachpyrs showed substantial peaks for free chelator, indicative of labilization that can be ascribed to a distorted coordination geometry ([Mn(tachpyr)]$^{2+}$) or to steric effects of *N*-alkylation, respectively (see below).

Electronic structure

Solution-phase magnetic susceptibilities and vis-near IR spectra were measured to confirm the oxidation states of the complexes, to define their spin states, and to investigate the effects of *N*-alkylation on the ligand-field strength of tachpyr (Table 1). Magnetic moments of **1b**–**4c** were determined in DMSO solution using Evans's method (Table 1).[13,14] The data fully support the assignment of the d^5-HS, d^7-HS, d^8 and d^9 electron configurations respectively to all Mn(II), Co(II), Ni(II), and Cu(II) complexes. A magnetic moment determination of **1a** was not possible due to oxidation processes,[15,16] but the similarity of its spectra to **1b** and **1c** support the Co(II)-HS formulation.

The influence of chelators on electronic states was further examined by visible-near IR (350–1200 nm) spectroscopy in MeCN solvent (Table 1). A straightforward assignment of absorption bands may be made in most if not all cases. The absorption bands of Co(II) compounds **2** at *ca.* 1050 and 510 nm are assigned to $^4T_{1g}\longrightarrow{}^4T_{2g}(F)$ and $^4T_{1g}\longrightarrow{}^4T_{1g}(P)$ transitions, respectively. We observe broadening or splitting of the higher-energy band, attributed to spin-orbit splitting of the $^4T_{1g}(P)$ state.[19] The Ni(II) compounds **3** exhibit two principal bands, at 800–950 and 500–600 nm; the third band at *ca.* 300 nm probably lies under a charge-transfer band of the ligand. The two components of the low-energy band are attributed to spin-orbit splitting of the $^3T_{2g}(F)$ state, giving rise to a spin-forbidden $^3A_{2g}$ $^1E_g(D)$ transition.[20] The visible-near IR spectra of **4a**–**4c** have a very broad single absorption maximum near 700 nm, as is typical for tetragonally-distorted six-coordinate Cu(II)N$_6$ complexes.[21]

In total, the electronic structures of the complexes indicate that *N*-alkylation of the tachpyr ligand weakens the metal–ligand interactions. The energies of the bands uniformly decrease in the ligand order tachpyr > (N–Me)$_3$tachpyr > (N–Et)$_3$tachpyr, indicating smaller d-orbital splittings as the amino H of tachpyr is replaced with bulkier groups (Table 1). Alkyl groups at the amino N of tachpyr clearly exert a steric influence on metal-binding by these nitrogens.

Structural studies

To elucidate the influences of the metal ion and chelator upon bonding in the complexes, we undertook crystallographic studies. A summary of structural parameters is presented in Table 2, and views of the metal complex cations are shown in Figs. 1–5.

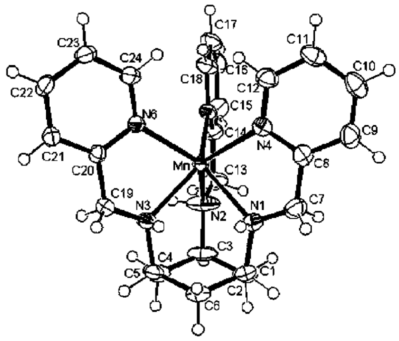

Fig. 1 ORTEP view of the complex cation of [Mn(tachpyr)](ClO$_4$)$_2$ (**1a**) with thermal ellipsoids at 50% probability.

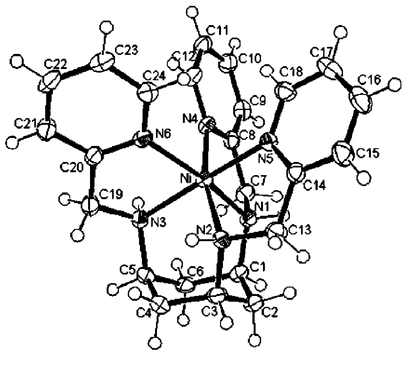

Fig. 2 ORTEP view of the complex cation of [Ni(tachpyr)](Cl)$_2$·CH$_3$OH (**3a**·MeOH) with thermal ellipsoids at 50% probability.

The M–N bond lengths of the complexes correlate reasonably well with ionic radii of M(II). As the six-coordinate ionic radius[22,23] increases from Ni(II) (0.83 Å) to Zn(II) (0.88 Å) and then to Mn(II) (0.97 Å), the average bond length of M–N(tach)

Table 1 Visible-near IR spectra and magnetic moments of Mn(II), Co(II), Ni(II), Cu(II), and Zn(II) complexes of tachpyr, (N–Me)$_3$tachpyr and (N–Et)$_3$tachpyr, plus selected reference compounds

	λ/nm[a]	ε/cm^{-1} M^{-1}	Assignment	μ_{eff}/BM[b]	Color
[Mn(tachpyr)](ClO$_4$)$_2$	—			5.7	None
[Mn((N–Me)$_3$tachpyr)](ClO$_4$)$_2$	—			5.8	None
[Mn((N–Et)$_3$tachpyr)](ClO$_4$)$_2$	—			5.8	None
[Co(tachpyr)](ClO$_4$)$_2$[c]	927	3.8	$^4T_{1g} \longrightarrow {}^4T_{2g}(F)$		Brown
	464, 546 sh	49	$^4T_{1g} \longrightarrow {}^4T_{1g}(P)$		
[Co((N–Me)$_3$tachpyr)](NO$_3$)$_2$[d]	1022	7.74	$^4T_{1g} \longrightarrow {}^4T_{2g}(F)$	4.0	Pink
	491, 552 sh	43.9	$^4T_{1g} \longrightarrow {}^4T_{1g}(P)$		
[Co((N–Et)$_3$tachpyr)](ClO$_4$)$_2$	1062	3.41	$^4T_{1g} \longrightarrow {}^4T_{2g}(F)$	4.1	Pink
	513	90.4	$^4T_{1g} \longrightarrow {}^4T_{1g}(P)$		
[Ni(tachpyr)](Cl)$_2$[d]	880 sh, 797	11.8,	$^3A_{2g} \longrightarrow {}^1E_g(D)$,		
	511	16.0	$^3A_{2g} \longrightarrow {}^3T_{2g}(F)$	2.9	Violet
		16.6	$^3A_{2g} \longrightarrow {}^3T_{1g}(F)$		
[Ni((N–Me)$_3$tachpyr)](ClO$_4$)$_2$	924, 812 sh	13.4,	$^3A_{2g} \longrightarrow {}^1E_g(D)$,		
		8.6	$^3A_{2g} \longrightarrow {}^3T_{2g}(F)$	3.0	Violet
	561	14.8	$^3A_{2g} \longrightarrow {}^3T_{1g}(F)$		
[Ni((N–Et)$_3$tachpyr)](ClO$_4$)$_2$	956, 820 sh	14.1,	$^3A_{2g} \longrightarrow {}^1E_g(D)$,		
	573	8.5	$^3A_{2g} \longrightarrow {}^3T_{2g}(F)$	3.0	Violet
		16.4	$^3A_{2g} \longrightarrow {}^3T_{1g}(F)$		
[Cu(tachpyr)](ClO$_4$)$_2$[6]	662	93.0	$^2E_g \longrightarrow {}^2T_{2g}$	1.6	Blue
[Cu((N–Me)$_3$tachpyr)](ClO$_4$)$_2$	723	81.4	$^2E_g \longrightarrow {}^2T_{2g}$	1.5	Blue
[Cu((N–Et)$_3$tachpyr)](ClO$_4$)$_2$	734	85.9	$^2E_g \longrightarrow {}^2T_{2g}$	1.6	Blue
[Co(tacnpyr)]$^{2+}$	886	24	$^3A_{2g} \longrightarrow {}^1E_g(D)$		
[Ni(tacnpyr)]$^{2+}$ [e] [17]	810	36	$^3A_{2g} \longrightarrow {}^3T_{2g}(F)$		
	515	27	$^3A_{2g} \longrightarrow {}^3T_{1g}$		
[Cu(tacnpyr)]$^{2+}$ [18]	695	121	$^2E_g \longrightarrow {}^2T_{2g}$		

[a] MeCN solvent unless otherwise indicated. [b] 1.5×10^{-2} M in DMSO-d$_6$. [c] Optical spectrum in water. [d] Optical spectrum in MeOH solvent. [e] tacnpyr = *N*,*N′*,*N″*-tris(2-pyridylmethyl)-[9]aneN$_3$.

Table 2 Structural parameters of Mn(II), Ni(II), Cu(II) and Zn(II) complexes of tachpyr and (N–Me)$_3$tachpyr, and other compounds (Scheme 2)

	Ionic radius[22,23]/Å	M–N(tach or other amine) bond distance/Å	M–N(pyridyl) bond distance/Å	Twist angle, a[a]/°
[Mn(tachpyr)]$^{2+}$ (**1a**)	0.97	2.2330(17)	2.2829(17)	2.5(1)
		2.236(2)	2.2920(18)	
		2.245(2)	2.2992(17)	
[Ni(tachpyr)]$^{2+}$ (**3a**)	0.83	2.099(4)	2.118(4)	45.5(2)
		2.099(4)	2.122(4)	
		2.107(4)	2.127(4)	
[Cu(tachpyr)]$^{2+}$ (**4a**)[6]	0.87	2.245(5)	2.458(5)	
		2.033(5)	2.032(5)	
		2.099(5)	2.053(5)	
[Zn(tachpyr)]$^{2+}$ (**5a**)[7]	0.88	2.160(3)	2.165(4)	43.7(2)
[Ni((N–Me)$_3$tachpyr)]$^{2+}$ (**3b**)	0.83	2.159(4)	2.106(3)	48.1(3)
		2.170(4)	2.107(4)	
		2.172(4)	2.108(3)	
[Cu((N–Me)$_3$tachpyr)]$^{2+}$ (**4b**)	0.87	2.325(4)	2.336(4)	44.9(1)
		2.091(4)	2.067(4)	
		2.159(4)	2.071(4)	
[Zn((N–Me)$_3$tachpyr)]$^{2+}$ (**5b**)	0.88	2.228(2)	2.165(2)	43.19(8)
fac-[Ni(ampy)$_3$]$^{2+}$ [b] [24]	0.83	2.13(2)	2.07(2)	
[Ni(tach)$_2$]$^{2+}$ [25]	0.83	2.131(3)		
		2.134(2)		
[Ni(tacnpyr)]$^{2+}$ [17]	0.83	2.108(4)	2.034(4)	46.8
		2.111(4)	2.051(4)	
		2.078(4)	2.108(4)	
mer-[Zn(ampy)$_3$]$^{2+}$ [26]	0.88	2.143(5)	2.215(5)	
fac-[Mn(ampy)$_3$]$^{2+}$ [27]	0.97	2.266(6)	2.266(5)	
[Mn(tacnpyr)]$^{2+}$ [17]	0.97	2.278(6)	2.207(5)	19.6
		2.291(5)	2.203(6)	
		2.286(6)	2.229(6)	
[Cu(tach)$_2$]$^{2+}$ [25]	0.87	2.353(7)		
		2.078(6)		

[a] Fig. 6; average of up to three values, whose range is less than 1° in all cases except **4b**. [b] ampy = 2-(aminomethyl)pyridine.

and the average bond length of M–N(pyridyl) increase proportionally. The M–N distances of [M(tachpyr)]$^{2+}$ are generally similar to those of other aminopyridyl ligands (Table 2 and Scheme 2). The Mn(II)–N distances of **1a** range from 2.2330(17) to 2.2992(17) Å, a span that covers all Mn–N distances of *fac*-[Mn(ampy)$_3$]$^{2+}$ (ampy = 2-(aminomethyl)pyridine)[27] and [Mn(tacnpyr)]$^{2+}$ (tacnpyr = *N*,*N′*,*N″*-tris(2-pyridylmethyl)-[9]aneN$_3$).[17] The shortest Ni–N distances of **3a** are somewhat longer than the shortest Ni–N distances of [Ni(tacnpyr)]$^{2+}$ [2.099(4) *vs.* 2.034(4) Å] (Table 1).

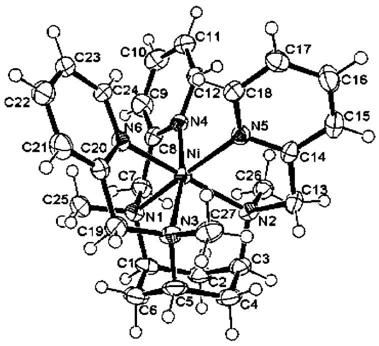

Fig. 3 ORTEP view of the complex cation of [Ni((N–Me)$_3$-tachpyr)](ClO$_4$)$_2$·MeCN (**3b**·MeCN) with thermal ellipsoids at 50% probability.

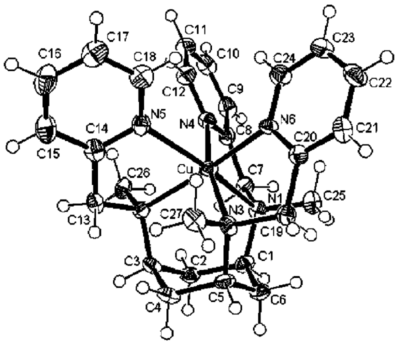

Fig. 4 ORTEP view of the complex cation of [Cu((N–Me)$_3$-tachpyr)](ClO$_4$)$_2$ (**4b**) with thermal ellipsoids at 50% probability.

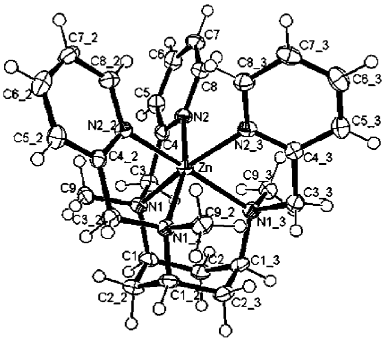

Fig. 5 ORTEP view of the complex cation of [Zn((N–Me)$_3$-tachpyr)](ClO$_4$)$_2$ (**5b**) with thermal ellipsoids at 50% probability.

The M–N(tach) bond lengths in [M((N–Me)$_3$tachpyr)]$^{2+}$ are overall longer than those of [M(tachpyr)]$^{2+}$ [M = Ni(ɪɪ), Zn(ɪɪ)], a difference clearly attributable to the steric effect of *N*-alkylation in tachpyr. Thus, the M–N(tach) bonds are *ca.* 0.06 Å longer than M–N(pyridyl) ones in [Ni((N–Me)$_3$tachpyr)]$^{2+}$ and [Zn((N–Me)$_3$tachpyr)]$^{2+}$, but the M–N(tach) and M–N(pyridyl) bond distances do not differ significantly in [Ni(tachpyr)]$^{2+}$ and [Zn(tachpyr)]$^{2+}$ (Table 2). The Mn(ɪɪ)–N(pyridyl) distances substantially exceed the Mn(ɪɪ)–N(tach) distances. This is ascribed to the large ionic radius of Mn(ɪɪ), which does not allow the pendant arms to fully surround it and leads to other structural differences described below.

The bond distances of the Cu(ɪɪ) derivatives (**4a**,**4b**) are irregular and indicative of Jahn–Teller distortion.[21] The extent of distortion in **4a** and **4b** is typical of Cu(ɪɪ)N$_6$ compounds. It is measured by the tetragonality, defined as the mean of Cu–N distances in the square plane divided by the mean of the axial Cu–N bond lengths.[28] The tetragonalities of **4a** and **4b** are 0.87 and 0.90, respectively, comparable to 0.87 in [Cu([9]aneN$_3$)$_2$](BPh$_4$)$_2$[29] and 0.88 in [Cu(tach)$_2$](ClO$_4$)$_2$.[25]

Tachpyr and *N*-alkylated tachpyr innately prefer an octahedral coordination geometry, but the structure of [Mn(tachpyr)](ClO$_4$)$_2$ (**1a**) is nearly trigonal-prismatic, as demonstrated by twist angles (Table 2; Fig. 6). This may be attributed to the large size of high-spin Mn(ɪɪ) and its lack of a geometry preference derived from ligand field stabilization energy, coupled with constraints on edge lengths of the MN$_6$ coordination polyhedron enforced by coordinated tachpyr. The cyclohexyl ring of [M(tachpyr)]$^{2+}$ holds the tach-amine nitrogens to a regular triangle with a *ca.* 3.0 Å side, and the CH$_2$-2-pyridyl pendant groups constrain the distance between pyridyl-N and associated tach-N donors to *ca.* 2.7 Å.[7,12] Thus, when edge lengths of the MN$_6$ coordination polyhedron are constrained, a trigonal prism provides a better fit to a larger metal ion because it possesses longer M–N bonds than an octahedron.[28]

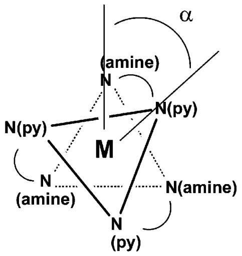

Fig. 6 The twist angle, *α*, defined for the MN$_6$ coordination sphere.

The trigonal-prismatic geometry of **1a** is accompanied by a marked distortion of coordinated amino groups. Tachpyr and derivatives prefer to bind octahedrally because metal coordination to the tach N atoms constrains the three N–CH$_2$py bond vectors to orient in a mutually clockwise or counterclockwise direction about the C_3 axis. This gives the Λ or Δ conformation of the pseudo-octahedral geometry that is typically observed for [M(tachpyr)]$^{2+}$.[12] In **1a**, the tach N atoms would therefore be distorted toward a planar geometry of the non-hydrogen substituents, for example, a planar disposition of C3, C13 and Mn about N2 (Fig. 1). Close examination of the ellipsoids of the tach N atoms indicates elongation normal to the plane of the non-hydrogen substituents, suggestive of a crystallographic disorder. Thus the observed nitrogen position appears to be an average of two inverse pyramidal conformations. The pendant arms of **1a** are also spread out to further lengthen the Mn(ɪɪ)–N(pyridyl) bond distances relative to the Mn(ɪɪ)–N(amino) distances (Table 2).

Conclusion

The tripodal aminopyridyl chelators tachpyr and (N–R)$_3$-tachpyr demonstrate a strong preference for octahedral coordination geometry and for divalent metal ions of six-coordinate ionic radius 0.8–0.9 Å, based on solution and solid-state characterization of Co(ɪɪ), Ni(ɪɪ), Cu(ɪɪ), and Zn(ɪɪ) complexes. The steric effect of R is pronounced in solution and solid-state properties of (N–R)$_3$tachpyr derivatives. Owing to the large size and lack of coordination geometry preferences in the Mn(ɪɪ) ion, [Mn(tachpyr)](ClO$_4$)$_2$ has a trigonal-prismatic coordination geometry with severe distortions of coordinated amino groups. The poor match is also reflected in the solution-phase lability of [Mn(tachpyr)]$^{2+}$. The findings indicate that tachpyr may be an effective chelator of smaller divalent metal ions. Studies of further tach derivatives and relationships of structure and solution properties are currently underway.

Experimental

General

All the materials listed below were of a research grade or a spectro-quality grade in the highest purity available and were generally used without further purification except Et_2O. Et_2O was distilled from Na and used immediately. Anhydrous grade DMF, MeOH, CH_3CN, and *t*-butanol and the salts $Zn(ClO_4)_2$·$6H_2O$, $Cu(ClO_4)_2$·$6H_2O$, $NiCl_2$·$6H_2O$, $Ni(ClO_4)_2$·$6H_2O$, $Co(NO_3)_2$·$6H_2O$, $Co(ClO_4)_2$·$6H_2O$ and $Mn(ClO_4)_2$·$6H_2O$ were obtained from Aldrich. Anhydrous grade EtOH was obtained from Pharmco. DMSO-d_6, and CH_3CN-d_3 were obtained from Cambridge Isotope Laboratories. All of the UV-Vis electronic spectra were measured using a Varian Cary 5 or Varian Cary 50-Bio UV-vis spectrometer with 1 or 3 cm^3 quartz cuvettes (1 cm path-length). Fast atom bombardment (FAB-MS) mass spectra were taken on an Extrel 4000. Samples were desorbed from mixtures of glycerol, thioglycerol ('TG'), DMSO, nitrobenzyl alcohol ('NBA') or Magic Bullet ('MB', a 3:1 mixture of dithiothreitol and dithioerythritol) as indicated. The required ion mass was calculated using the program developed by Scientific Instrument Services (http://www.sisweb.com/cgi-bin/mass10.pl). ^1H and ^{13}C NMR spectra were obtained using a Bruker AM360 instrument. Chromatograms (RP-HPLC) were obtained on a Waters 600E/486/746 dual-pump system with UV detection at 254 and 280 nm. A Beckman Ultrasphere 4.6 × 25 cm RP-18 column was eluted with a gradient of 100% 0.05 M Et_3N·HOAc buffer (pH = 5.5) to 100% MeOH over 25 min. Magnetic moment was measured by Evans's method[13,30] ($Q = 2$ and $\nu_I = 360 \times 10^6$), DMSO-d_6 as a solvent, and *t*-butanol as an indicator. Elemental analysis was performed by Atlantic Microlabs (Atlanta, Georgia). Tachpyr,[31] (N–Me)$_3$tachpyr,[9] (N–Et)$_3$tachpyr[9] and complexes **4a**[6] and **5a**[7] were prepared as reported. Isolated solids were washed with *ca.* 2 cm^3 of the indicated solvent; unless otherwise stated, and recrystallization was accomplished by vapor-phase diffusion of Et_2O into a solution of crude material in MeCN or MeOH (*ca.* 1 cm^3). Drying was accomplished in air or under reduced pressure (*ca.* 10^{-2} Torr) with a standard Schlenk line. Anaerobic manipulations were accomplished by Schlenk techniques.

Caution: perchlorate salts can be explosive and should be handled with care.

[Mn(tachpyr)](ClO_4)$_2$ (1a)

A yellow solution of tachpyr (0.120 g, 0.299 mmol) in MeOH (2 cm^3) was added to a solution of $Mn(ClO_4)_2$·$6H_2O$ (0.108 g, 0.299 mmol) in MeOH (2 cm^3). Yellow prisms formed after 20 min and were isolated and washed with MeOH (1 cm^3). Slow diffusion of Et_2O into an MeCN solution of the complex provided pale yellow prisms (suitable for X-ray crystallography prior to drying) that were isolated and dried to a pale yellow solid (0.138 g, 70.5%). (Found: C, 44.55; H, 4.30; N, 13.70. $C_{24}H_{30}Cl_2MnN_6O_8$·1/2MeCN requires: C, 44.36; H, 4.69; N, 13.45%.) MS (FAB/NBA/DMSO): *m*/*z* 556 (M − ClO_4^-), 455 (M). μ_{eff} = 5.7 BM at 25 °C.

[Mn((N–Me)$_3$tachpyr)](ClO_4)$_2$ (1b)

A yellow solution of (N–Me)$_3$tachpyr (0.0726 g, 0.163 mmol) in a mixture of MeOH/Et_2O (2 cm^3/4 cm^3) was added to a solution of $Mn(ClO_4)_2$·$6H_2O$ (0.0590 g, 0.163 mmol) in a mixture of MeOH/Et_2O (2 cm^3/4 cm^3). The yellow-white precipitate was isolated and dried to a pale yellow solid. This was washed with MeOH and Et_2O and dried under reduced pressure affording a pale yellow solid (0.072 g, 63.2%). Pale yellow crystals were obtained by Et_2O diffusion into an MeCN solution of the complex. (Found: C, 46.20; H, 5.15; N, 11.96. $C_{27}H_{36}Cl_2MnN_6O_8$ requires: C, 46.43; H, 5.20; N, 12.03%.) MS (FAB/DMSO/glycerol): *m*/*z* 598 (M − ClO_4^-), 445 (L). μ_{eff} = 5.8 BM at 25 °C.

[Mn((N–Et)$_3$tachpyr)](ClO_4)$_2$ (1c)

A brown solution of (N–Et)$_3$tachpyr (0.0590 g, 0.121 mmol) in a mixture of MeOH/Et_2O (2 cm^3/6 cm^3) was added to a solution of $Mn(ClO_4)_2$·$6H_2O$ (0.0438 g, 0.121mmol) in a mixture of MeOH/Et_2O (2 cm^3/4 cm^3) affording a yellow-brown solution. Addition of excess Et_2O provided a brown precipitate that was isolated and dried to a pale brown solid. This was washed with CH_2Cl_2, dissolved in MeCN and subjected to vapor-phase diffusion of Et_2O giving pale brown prisms. They were isolated and dried to a pale brown solid (0.0437 g, 48.8%). (Found: C, 48.54; H, 5.68; N, 11.29. $C_{30}H_{42}Cl_2MnN_6O_8$ requires: C, 48.66; H, 5.72; N, 11.35%.) MS (FAB/MB): *m*/*z* 640 (M − ClO_4^-), 487 (L). μ_{eff} = 5.8 BM at 25 °C.

[Co(tachpyr)](ClO_4)$_2$ (2a)

Under an N_2 atmosphere using N_2-purged MeOH, a pale pink solution of $Co(ClO_4)_2$·$6H_2O$ (2.26×10^{-2} g, 6.18×10^{-5} mol, in 0.75 cm^3 MeOH) was added to a pale yellow solution of tachpyr (2.52×10^{-2} g, 6.25×10^{-5} mol, in 0.75 cm^3 MeOH), giving a pink-mauve solution that formed tan microcrystals within 3 min. After standing for 24 h, the supernatant was decanted and the solid dried. Vapor-phase diffusion of Et_2O into an MeCN (0.75 cm^3) solution of this solid afforded bronze prisms (2.01×10^{-2} g, 49%). (Found: C, 43.55; H, 4.57; N, 12.85. $C_{24}H_{30}Cl_2CoN_6O_8$ requires: C, 43.65; H, 4.58; N, 12.73%.) MS (FAB, DMSO/glycerol): *m*/*z* 460 (M^{2+} − H^+). HPLC: R_t = 11.17 min ([Co(tachpyr)]$^{2+}$), 3.34 min (Co^{III} complex). Oxidation-sensitivity of the complex precluded a magnetic moment determination. λ_{max}/nm (H_2O) 927 (ε/cm^{-1} M^{-1} 3.8), 464 (49), 546 (shoulder).

[Co((N–Me)$_3$tachpyr)](NO_3)$_2$ (2b)

A yellow solution of (N–Me)$_3$tachpyr (0.1062 g, 2.39×10^{-4} mol) in MeOH/Et_2O (2cm^3/4cm^3) solvent was added to a pink solution of $Co(NO_3)_2$·$6H_2O$ (0.0695 g, 2.39×10^{-4} mol) in a mixture of MeOH/Et_2O (2 cm^3/4 cm^3), affording a pink precipitate. Et_2O (12 cm^3) was added to complete precipitation and the solid isolated and dried to a pink powder. This was washed with MeCN and Et_2O and dried to a pink solid that was characterized (0.1012 g, 67.5%). Pink crystals were later obtained by Et_2O diffusion into a MeOH solution. (Found: C, 51.50; H, 5.70; N, 17.69. $C_{27}H_{36}CoN_8O_6$ requires: C, 51.68; H, 5.78; N, 17.86%.) MS (FAB/DMSO/glycerol/H_2O): *m*/*z* 503 (M − $2NO_3^-$). μ_{eff} = 4.0 BM at 25 °C. λ_{max}/nm (MeOH) 1032 (ε/cm^{-1} M^{-1} 7.53), 493 (38.01), and 552 (19.18).

[Co((N–Et)$_3$tachpyr)](ClO_4)$_2$ (2c)

A brown solution of (N–Et)$_3$tachpyr (0.0730 g, 1.50×10^{-4} mol) in MeOH/Et_2O (2 cm^3/6 cm^3) was added to a pink solution of $Co(ClO_4)_2$·$6H_2O$ (0.0549 g, 1.50×10^{-4} mol) in MeOH/Et_2O (2 cm^3/6 cm^3) affording a peach precipitate. The precipitate was isolated and dried to a peach solid. This was washed with MeOH (5 cm^3) and dried to a peach solid that was characterized (0.0791 g, 70.9%). Pale pink crystals were later obtained by Et_2O diffusion into an MeCN solution. (Found: C, 48.08; H, 5.74; N, 11.14. $C_{30}H_{42}Cl_2CoN_6O_8$ requires: C, 48.40; H, 5.69; N, 11.29%.). MS (FAB/DMSO/NBA): *m*/*z* 545 (M − $2ClO_4^-$). μ_{eff} = 4.1 BM at 25 °C. λ_{max}/nm (MeCN) 1062 (ε/cm^{-1} M^{-1} 3.41), 513 (90.4).

[Ni(tachpyr)]Cl_2 (3a)

A pale yellow-brown solution of tachpyr (0.0888 g, 0.220 mmol) in MeOH (2 cm^3) was added to a green solution of $NiCl_2$·$6H_2O$ (0.0524 g, 0.220 mmol) in MeOH (2 cm^3). The mixture formed a brown solution immediately. By diffusing Et_2O into the mixture, purple prisms (a MeOH solvate suitable for X-ray crystallography prior to drying) and a brown precipitate formed. The crystals were separated from the precipitate manually, washed with Et_2O, and dried giving a purple solid (0.034 g, 34.7%) (Found: C, 51.65; H, 5.97; N, 14.79.

$C_{24}H_{30}Cl_2N_6Ni{\cdot}3/2H_2O$ requires: C, 51.55; H, 5.95; N, 15.03%.) MS (FAB/MB/DMSO): *m*/*z* 461 (M − 2Cl), 495 (M − Cl). HPLC: R_t = 8.47 min. μ_{eff} = 2.9 BM at 25 °C. λ_{max}/nm (MeOH) 880 (ε/cm^{-1} M^{-1} 11.8), 797 (16.0), 511 (16.6).

[Ni(tachpyr)](ClO_4)$_2$ (3a′)

A yellow solution of tachpyr (0.0296 g, 7.35 × 10^{-5} mol) in MeOH (2 cm^3) was added to a green solution of Ni(ClO_4)$_2$·6H_2O (0.0202 g, 7.35 × 10^{-5} mol) in MeOH (2 cm^3), affording a pale lavender solution. A layer of Et_2O (*ca.* 5 cm^3) was added producing a yellow precipitate after standing for 30 min. The precipitate was washed with MeOH (5 cm^3) and the remaining pale pink solid recrystallized from MeCN (2 cm^3) by vapor-phase diffusion of Et_2O. A 55% yield (0.267 g, 4.04 × 10^{-5} mol) of pink microcrystals was obtained. (Found: C, 43.35; H, 4.48; N, 12.69. $C_{24}H_{30}Cl_2N_6NiO_8$ requires: C, 43.67; H, 4.58; N, 12.73%.) Other spectroscopic properties were identical to those of **3a**.

[Ni((N–Me)$_3$tachpyr)](ClO_4)$_2$ (3b)

A yellow solution of (N–Me)$_3$tachpyr (0.0663 g, 0.101 mmol) in MeOH (2 cm^3) was added to a green solution of Ni(ClO_4)$_2$·6H_2O (0.0546 g, 0.149 mmol) in MeOH (2 cm^3), forming pink microcrystals. After standing for 30 min, they were isolated, washed with cold MeOH, and dried giving a pale pink solid. Pink prisms suitable for X-ray crystallography were obtained by Et_2O diffusion into an MeCN solution of the complex. Crystals were isolated and dried under reduced pressure affording a purple solid (0.0604 g, 57.8%). (Found: C, 46.42; H, 5.21; N, 11.96. $C_{27}H_{36}Cl_2N_6NiO_8$ requires: C, 46.18; H, 5.17; N, 11.97%.) MS (FAB/glycerol): *m*/*z* 502 (M − 2ClO_4^-), 601 (M − ClO_4^-). μ_{eff} = 3.0 BM at 25 °C. λ_{max}/nm (MeCN) 925 (ε/cm^{-1} M^{-1} 3.4), 814 (8.8), 562 (15.4).

[Ni((N–Et)$_3$tachpyr)](ClO_4)$_2$ (3c)

To a green solution of Ni(ClO_4)$_2$·6H_2O (0.0445 g, 0.121 mmol) in a mixture of EtOH/Et_2O (2 cm^3/4 cm^3) was added a brown solution of (N–Et)$_3$tachpyr (0.0591 g, 0.121 mmol) in a mixture of EtOH/Et_2O (2 cm^3/4 cm^3) affording a peach precipitate immediately. This was isolated, dried under reduced pressure, washed with MeOH and Et_2O, and taken up into MeCN. Pale purple prisms were obtained by Et_2O diffusion into an MeCN solution of the complex, isolated, and dried under reduced pressure affording a pale purple solid (0.0649 g, 72.1%). (Found: C, 48.14; H, 5.68; N, 11.25. $C_{30}H_{42}Cl_2N_6NiO_8$ requires: C, 48.41; H, 5.69; N, 11.29%.) MS (FAB/DMSO/NBA): *m*/*z* 544 (M − 2ClO_4^-), 643 (M − ClO_4^-). μ_{eff} = 3.0 BM at 25 °C. λ_{max}/nm (MeCN) 944 (ε/cm^{-1} M^{-1} 14.2), 818 (8.6), 574 (16.4).

[Cu((N–Me)$_3$tachpyr)](ClO_4)$_2$ (4b)

A yellow solution of (N–Me)$_3$tachpyr (0.0769 g, 0.173 mmol) in EtOH (2 cm^3) was added to blue Cu(ClO_4)$_2$·6H_2O (0.0641 g, 0.173 mmol) in EtOH (3 cm^3), forming a blue precipitate. Addition of Et_2O (10 cm^3) yielded a further precipitate which was isolated and dried to a blue solid. This was washed with MeOH (6 cm^3), dissolved in MeCN (*ca.* 10 cm^3), filtered, and dried under reduced pressure to a blue solid (0.0485 g, 58.2%). Et_2O diffusion into a DMF solution provided single crystals suitable for X-ray study. (Found: C, 45.78; H,4.74; N, 12.08. $C_{27}H_{36}Cl_2CuN_6O_8$ requires: C, 45.86; H, 5.13; N, 11.89%.) MS (FAB/glycerol): *m*/*z* 507 (M − 2ClO_4^-), 608 (M − ClO_4^-). μ_{eff} = 1.5 BM at 25 °C. λ_{max}/nm (MeCN) 723 (ε/cm^{-1} M^{-1} 81.4).

[Cu((N–Et)$_3$tachpyr)](ClO_4)$_2$ (4c)

A brown solution of (N–Et)$_3$tachpyr (0.0723 g, 0.149 mmol) in EtOH/Et_2O (2 cm^3/4 cm^3) was added to a pale blue solution of Cu(ClO_4)$_2$·6H_2O (0.0550 g, 0.149 mmol) in EtOH/Et_2O (2 cm^3/4 cm^3) forming a gray-blue precipitate, which was isolated and dried to a pale blue solid. This was washed with EtOH (5 cm^3) and crystallized by Et_2O vapor diffusion to an MeCN solution, giving pale green cubes and dark green powder. Crystals were collected manually, washed with MeOH, redissolved in MeCN, and recrystallized by the same procedure giving pale green cubes. After decanting the supernatant, the crystals were dried to a pale green solid (0.0609 g, 54.6%). (Found: C, 47.81; H, 5.58; N, 11.21. $C_{30}H_{42}Cl_2CuN_6O_8$ requires: C, 48.10; H, 5.65; N, 11.22%.) MS (FAB/DMSO/NBA): *m*/*z* 549 (M − 2ClO_4^-), 649 (M − ClO_4^-). μ_{eff} = 1.6 BM at 25 °C. λ_{max}/nm (MeCN) 734 (ε/cm^{-1} M^{-1} 85.9).

[Zn((N–Me)$_3$tachpyr)](ClO_4)$_2$ (5b)

A yellow solution of (N–Me)$_3$tachpyr (0.0387 g, 0.0870 mmol) in MeOH (3 cm^3) was added to Zn(ClO_4)$_2$·6H_2O (0.0325 g, 0.087 mmol) in EtOH (2 cm^3), affording a light yellow precipitate. After standing for 1 h, the precipitate was isolated, washed with EtOH, and dried to a white solid (0.0403g, 56.6%). Et_2O diffusion into an MeCN solution yielded single crystals suitable for X-ray crystallography. (Found: C, 45.68; H, 5.20; N, 11.65. $C_{27}H_{36}Cl_2N_6O_8Zn$ requires: C, 45.75; H, 5.20; N, 11.65%.) ^{1}H NMR [360 MHz, $(CD_3)_2SO$, 25 °C]: δ 8.16, 7.63 (4H, t, m, C_5H_4N); 4.97, 3.68 [2H, d, d, N(CH_3)–C*H*$_2$–py]; 3.13 (1H, br s, *A*MM′XX′, cyclohexyl methine H atoms); 2.96 (1H, br d, AA′*M*X, equatorial cyclohexyl methylene H atoms, diastereotopic), 2.15 (1H, br d, AA′M*X*, axial cyclohexyl methylene H atoms, diastereotopic); 1.95 [3H, s, N(C*H*$_3$)–CH_2–py]. MS (FAB/glycerol): *m*/*z* 507 (M − 2ClO_4^-), 609 (M − ClO_4^-).

[Zn((N–Et)$_3$tachpyr)](ClO_4)$_2$ (5c)

A yellow solution of (N–Et)$_3$tachpyr (0.0798 g, 0.164 mmol) in MeOH (2 cm^3) was added to a Zn(ClO_4)$_2$·6H_2O (0.0612 g, 0.164 mmol) in MeOH (3 cm^3) affording a yellow-brown precipitate. Et_2O (12 cm^3) was added giving further precipitate that was isolated, washed with MeOH, and dissolved in MeCN and filtered. This was dried to a white solid that was characterized (0.0574 g, 40.7%); Et_2O diffusion into an MeCN solution provided colorless prisms. (Found: C, 47.63; H, 5.91; N, 11.12. $C_{30}H_{42}Cl_2N_6O_8Zn$ requires: C, 47.98; H, 5.64; N, 11.19%.) ^{1}H NMR (360 MHz, CD_3CN, 25 °C): δ 8.10, 8.06, 7.57, 7.53 (4H, d, t, d, t, C_5H_4N); 4.55, 4.09 [2H, d, d, N(CH_2CH_3)–C*H*$_2$–py]; 3.39 (1H, br s, *A*MM′XX′, cyclohexyl methine H atoms); 2.69 (1H, br d, AA′*M*X, equatorial cyclohexyl methylene H atoms, diastereotopic), 2.05 (1H, br d, AA′M*X*, axial cyclohexyl methylene H atoms, diastereotopic); 2.55, 1.97 [2H, m, m, N(C*H*$_2$$CH_3$)–$CH_2$, diastereotopic]; 0.87 [3H, dd, N(CH_2C*H*$_3$)]. ^{13}C NMR (CD_3CN, 25° C): δ 161.18, 152.83, 146.02, 131.17, 130.52 (C_5H_4N); 59.47 [N(CH_2CH_3)–*C*H$_2$–py]; 57.11 (1C, cyclohexyl methane C atoms); 53.43 [N(*C*H$_2$$CH_3$)–$CH_2$–py]; 32.70 (cyclohexyl methylene C atoms); 9.98 [N(CH_2*C*H$_3$)–CH_2–py]. MS (FAB/glycerol/DMSO): *m*/*z* 549 (M − 2ClO_4^-), 651 (M − ClO_4^-).

X-Ray data collection, structure solution and refinement for metal complexes

Single crystals suitable for X-ray crystallography of metal complexes were grown by Et_2O diffusion into solutions of the corresponding metal complexes in MeOH, CH_3CN, DMF, or DMSO. Single crystals were mounted on fibers and transferred to the goniometer. The crystals were cooled to −100 °C during data collection with a stream of cold nitrogen gas. Data collection was made on a Siemens SMART diffractometer with a CCD area detector, using graphite monochromated MoKα radiation. The SHELXTL software, version 5, was used for solutions and refinement.[32] Absorption corrections were made with SADABS.[33] Molecules were refined by full-matrix least-squares on F^2. The twist angles *α* (Fig. 6) were calculated by setting a centroid in each of the triangles of the three pyridyl nitrogens and of the three amino nitrogens (designated X1 and X2 in the structure data). Then, the torsion angles N(tach)–X1–X2–N(pyridyl), each involving the nitrogens of one chelate arm, were calculated and averaged. Compound **5b** has crystallographically imposed 3-fold symmetry with the Zn atom on a 3-fold axis. ORTEP drawings were made with SHELXTL[32] and ORTEP-3.[34,35]

Crystal/refinement data

[Mn(tachpyr)][ClO$_4$]$_2$ (1a). $C_{24}H_{30}Cl_2MnN_6O_8$, M = 656.38, monoclinic, space group $P2_1/c$, a = 13.4196(2), b = 13.8089(1), c = 15.2639(1) Å, β = 110.406(1)°, V = 2651.05(5) Å^3, D_c (Z = 4) = 1.645 g cm^{-3}, μ_{Mo} = 7.62 cm^{-1}, specimen 0.26 × 0.40 × 0.58 mm, N_t = 16529, N = 6119 (R_{int} = 0.0230), N_o = 5083 [$I > 2\sigma(I)$], R, $wR2$ (obs. data) = 0.0392, 0.1093, R, $wR2$ (all data) = 0.0485, 0.1144, $|\Delta\rho_{max}|$ = 0.766 e Å^{-3}.

[Ni(tachpyr)]Cl$_2$·CH$_3$OH (2a·CH$_3$OH). $C_{25}H_{34}Cl_2N_6NiO$, M = 564.19, monoclinic, space group $P2_1/n$, a = 9.4103(2), b = 14.5893(3), c = 19.1238(4) Å, β = 94.318(1)°, V = 2618.05(9) Å^3, D_c (Z = 4) = 1.431 g cm^{-3}, μ_{Mo} = 9.76 cm^{-1}, specimen 0.10 × 0.15 × 0.30 mm, N_t = 10411, N = 3757 (R_{int} = 0.0535), N_o = 3496 [$I > 2\sigma(I)$], R, $wR2$ (obs. data) = 0.0581, 0.1849, R, $wR2$ (all data) = 0.0619, 0.1938, $|\Delta\rho_{max}|$ = 1.418 e Å^{-3}.

[Ni((N–Me)$_3$tachpyr)][ClO$_4$]$_2$·MeCN (3b·MeCN). $C_{29}H_{39}Cl_2N_7NiO_8$, M = 743.28, triclinic, space group $P\bar{1}$, a = 9.9925(7), b = 10.2145(7), c = 18.1508(13) Å, α = 75.553(1), β = 86.028(1), γ = 61.606(1)°, V = 1575.6(2) Å^3, D_c (Z = 2) = 1.567 g cm^{-3}, μ_{Mo} = 8.48 cm^{-1}, specimen 0.08 × 0.10 × 0.18 mm, N_t = 10108, N = 7011 (R_{int} = 0.0323), N_o = 4168 [$I > 2\sigma(I)$], R, $wR2$ (obs. data) = 0.0612, 0.1125, R, $wR2$ (all data) = 0.1249, 0.1465, $|\Delta\rho_{max}|$ = 0.727 e Å^{-3}.

[Cu((N–Me)$_3$tachpyr)][ClO$_4$]$_2$ (4b). $C_{27}H_{36}Cl_2CuN_6O_8$, M = 707.06, monoclinic, space group $P2_1$, a = 9.4286(3), b = 17.1595(5), c = 9.6558(3) Å, β = 109.868(1)°, V = 1469.23(8) Å^3, D_c (Z = 2) = 1.598 g cm^{-3}, μ_{Mo} = 9.86 cm^{-1}, specimen 0.25 × 0.30 × 0.37 mm, N_t = 9397, N = 5523 (R_{int} = 0.0285), N_o = 4816 [$I > 2\sigma(I)$], R, $wR2$ (obs. data) = 0.0473, 0.1189, R, $wR2$ (all data) = 0.0561, 0.1287, $|\Delta\rho_{max}|$ = 1.291 e Å^{-3}.

[Zn((N–Me)$_3$tachpyr)][ClO$_4$]$_2$ (5b). $C_{27}H_{36}Cl_2N_6O_8Zn$, M = 708.89, trigonal, space group $P3_1c$, a = 11.2593(2), c = 13.5750(4) Å, V = 1490.37(6) Å^3, D_c (Z = 2) = 1.580 g cm^{-3}, μ_{Mo} = 10.64 cm^{-1}, specimen 0.10 × 0.12 × 0.30 mm, N_t = 9116, N = 2300 (R_{int} = 0.0373), N_o = 1986 [$I > 2\sigma(I)$], R, $wR2$ (obs. data) = 0.0275, 0.0542, R, $wR2$ (all data) = 0.0371, 0.0570, $|\Delta\rho_{max}|$ = 0.295 e Å^{-3}.

CCDC reference numbers 194166–194170.

See http://www.rsc.org/suppdata/dt/b2/b209228j/ for crystallographic data in CIF or other electronic format.

Acknowledgements

We thank Nole Whittaker (NIH/NIDDK) for expert mass spectroscopic work and Sujen Lai (UNH Chemistry) for dedicated synthetic studies.

References

1 A. B. Packard, J. F. Kronauge and M. W. Brechbiel, in *Topics in Biological Inorganic Chemistry*, M. J. Clarke and P. J. Sadler, ed., Springer-Verlag, New York, 1999, vol. 2, p. 45.
2 C. J. Anderson and M. J. Welch, *Chem. Rev.*, 1999, **99**, 2219.
3 R. Lauffer, *Chem. Rev.*, 1987, **87**, 901.
4 P. W. Durbin, B. Kullgren, J. Xu and K. N. Raymond, *Radiat. Prot. Dosim.*, 1998, **79**, 433.
5 N. C. Oboyle, G. P. Nicholson, T. J. Piper, D. M. Taylor, D. R. Williams and G. Williams, *Appl. Radiat. Isot.*, 1997, **48**, 183.
6 G. Park, E. Dadachova, A. Przyborowska, S.-J. Lai, D. Ma, G. Broker, R. Rogers, R. Planalp and M. Brechbiel, *Polyhedron*, 2001, **20**, 3155.
7 G. Park, N. Ye, R. Rogers, M. Brechbiel and R. Planalp, *Polyhedron*, 2000, **19**, 1155.
8 S. V. Torti, F. M. Torti, S. P. Whitman, M. W. Brechbiel, G. Park and R. P. Planalp, *Blood*, 1998, **92**, 1384.
9 G. Park, F. Lu, N. Ye, M. Brechbiel, S. Torti, F. Torti and R. Planalp, *JBIC, J. Biol. Inorg. Chem.*, 1998, **3**, 449.
10 R. P. Planalp, A. M. Przyborowska, G. Park, N. Ye, F. H. Lu, R. D. Rogers, G. A. Broker, S. V. Torti and M. W. Brechbiel, *Biochem. Soc. Trans.*, 2002, **30**, 758.
11 U. Brand and H. Vahrenkamp, *Inorg. Chim. Acta*, 1992, **198–200**, 663.
12 K. A. Hilfiker, R. D. Rogers, M. W. Brechbiel and R. P. Planalp, *Inorg. Chem.*, 1997, **36**, 4600.
13 D. F. Evans, *J. Chem. Soc.*, 1959, 2003.
14 D. Ostfeld and I. Cohen, *J. Chem. Ed.*, 1972, **49**, 829.
15 I. Bernal, F. Somoza, S. S. Massoud, N. M. Shuaib and H. M. R. Marafie, *J. Coord. Chem.*, 1996, **40**, 45.
16 N. Y. M. Iha, M. A. De Almeida Azzelini and S. Utsuno, *Polyhedron*, 1998, **17**, 3379.
17 K. Wieghardt, E. Schöffmann, B. Nuber and J. Weiss, *Inorg. Chem.*, 1986, **25**, 4877.
18 L. Christiansen, D. N. Hendrickson, H. Toftlund, S. R. Wilson and C.-L. Xie, *Inorg. Chem.*, 1986, **25**, 2813.
19 L. Banci, A. Bencini, C. Benelli, D. Gatteschi and C. Zanchini, *Struct. Bonding (Berlin)*, 1982, **52**, 37.
20 M. Elder, G. Prinz, P. Thornton and D. Busch, *Inorg. Chem.*, 1968, **7**, 2426.
21 B. Hathaway, R. Gillard and J. McCleverty, in *Comprehensive Coordination Chemistry*, G. Wilkinson, R. Gillard and J. McCleverty, ed., Pergamon, Oxford, 1987, vol. 5, ch. 53.4.
22 R. D. Shannon and C. T. Prewitt, *Acta Crystallogr., Sect. B*, 1969, **25**, 925.
23 R. Shannon, *Acta Crystallogr., Sect. A*, 1976, **32**, 751.
24 M. Niven and L. Nassimbeni, *Cryst. Struct. Comm.*, 1980, **9**, 227.
25 H. Ammeter, H. B. Bürgi, E. Gamp, V. Meyer-Sandrin and W. P. Jensen, *Inorg. Chem.*, 1979, **18**, 733.
26 M. Mikami-Kido and Y. Saito, *Acta Crystallogr., Sect. B*, 1982, **38**, 452.
27 D. J. Hodgson, K. Michelsen and E. Pedersen, *Acta Chem. Scand.*, 1990, **44**, 1002.
28 D. L. Kepert, *Inorganic Stereochemistry*, M. Becke, C. Jorgensen, M. Lappert, S. Lippard, J. Margrave, K. Niedenzu, R. Parry and H. Yamatera, ed., Springer-Verlag, Berlin, 1982, p. 92.
29 M. Kavana, D. R. Powell and J. N. Burstyn, *Inorg. Chim. Acta*, 2000, **297**, 351.
30 G. S. Girolami, T. B. Rauchfuss and R. J. Angelici, *Synthesis and Technique in Inorganic Chemistry: A Laboratory Manual*, University Science Books, Sausalito, CA, 1999.
31 T. Bowen, R. P. Planalp and M. W. Brechbiel, *Bioorg. Med. Chem. Lett.*, 1996, **6**, 807.
32 G. M. Sheldrick, SHELXTL, version 5.05, Siemens Analytical X-Ray Instruments Inc., Madison, WI, 1996.
33 G. M. Sheldrick, Program for Semiempirical Absorption Correction of Area Detector Data, University of Göttingen, Germany, 1996.
34 M. Burkitt, *Methods Enzymol.*, 1994, **234**, 66.
35 L. J. Farrugia, *J. Appl. Crystallogr.*, 1997, **30**, 565.